A Hybrid Unstructured Grid System for Viscous and Inviscid Aerodynamic Analysis

Akio Ochi and Eiji Shima
Kawasaki Heavy Industries, Ltd. (KHI)
1 Kawasaki-cho, Kakamigahara, 504-8710, Gifu, Japan
ochi_a@khi.co.jp and shima_e@khi.co.jp

Keywords: *CFD, Grid generation, Unstructured grid, Aerodynamic analysis*

Abstract

This paper describes a new hybrid unstructured grid system used in aerodynamic analysis using CFD. This new hybrid grid system is applicable both viscous and invscid flow analysis for complex geometry such as full configuration of airplanes. The volume grid of this hybrid grid system is created using in house automatic grid generator from a surface mesh that consists of quadrilateral and/or triangle cells. Volume grid cells near body surface consist of hexahedra and prism cells to perform viscous analysis. Starting from the surface mesh, grid generator piles up layers of volume cells like an expanding balloon. It takes a couple of hours to generate a three Million points grid system for an airplane with fuselage, wing, pylon, nacelle, horizontal and vertical tail wings.

This hybrid grid system has been applied various cases including highly complex geometry. Accuracy of the numerical results is validated for several aspects. This gird system has been used to develop aircrafts in our company.

1 Introduction

The principal motivation of this study is to apply an automatic grid generator to reduce total turn around time for CFD analysis. CFD analysis has been became more important tool to aerodynamic design. While aerodynamic designers demand more and more accurate analytical tools, turn around time of viscous analysis is too long to be practical tool. Because grid generation time has not been reduced compared to reduction of computation time that has been considerably reduced by development of numerical algorithms, increase of CPU performance, and parallel computing. Consequently, grid generation time becomes a dominant fraction. Even a well-trained engineer, it takes a couple of months to make a numerical grid for a full configuration aircraft with tails and/or engine nacelles and pylons.

We tried out several kinds of automatic grid generator. The automatic grid generation technique significantly reduced grid generation time from a couple of months to several hours. However it was found that tetrahedral cell and prism cell, which are usually utilized in automatic grid generation, often lose accuracy and resolution. Because spatial discretization for tetrahedral and prism cell have disadvantage to that for hexahedral cell. For aerodynamic analysis, losing accuracy produces non-physical entropy increase. It causes incorrect prediction of aerodynamic forces. In particular, drag component is very sensitive to non-physical entropy production. Lack of resolution around a leading edge section is not negligible for aerodynamic optimization of wing shapes.

Thus a new unstructured hybrid grid system and an automatic grid generator were developed for viscous/invscid aerodynamic analysis. This hybrid unstructured grid utilizes hexahedral volume cell around body surface to retain good accuracy.

2 Hybrid Grid System

The new hybrid grid system mainly consists of a large number of hexahedral and prism volume cells. Hexahedral volume cell is generated from quadrilateral surface cell. Prismatic volume cell is generated from triangle

surface cell. A small number of pyramid and tetrahedron cells are used as a link between hexahedral cells and prism cells. Number of cells and Fraction of cell types for specific case are shown in Table 1. Surface grid consists of combination of quadrilaterals and triangles. Hexahedral volume cell has a good property to obtain higher accuracy and higher resolution. In particularly, Quadrilateral surface mesh has a benefit for anisotropic shape such as leading and trailing edge sections in wing. If triangle cell is used, the number of surface grid points should be considerably increased to achieve same resolution and accuracy. On the other hand, triangular surface mesh is suitable for automatic surface mesh generation.

3 Grid Generation

The hybrid grid in this study is generated by a grid generator PUFGG (Pile-Up Forming Grid Generator) from surface grids. PUFGG is an automatic volume grid generator developed by Kawasaki. Surface grids are made using CATIA or other CAD systems. One of the advantages of PUFGG is that it is capable to generate volume grid from mixed quadrilateral and triangular surface cells.

PUFGG generates the volume grid starting from a surface grid and piles up layers. Figure 1 shows a growing volume grid in process of grid generation for a wind tunnel test model called ONERA calibration model M5. Volume grid grows up like balloon inflation as shown in Fig.1. Near the body surface, hexahedral and prism cells will be created from quadrilateral and triangular surface cells, respectively. In this case all surface mesh cells consist of quadrilateral cells as show in Fig. 2. In the off body region, grid cells are merged to reduce the number of grid cells. Figure 3 is a cross section of numerical grid at a half semi-span location. Grid generation time is about a half-hours for this configuration. It takes about two hours for full configuration (wing-body, horizontal and vertical tails, engine nacelle, and pylon) using PC.

However grid generation using piling up approach often breaks for complex geometry, because deep concave surface shape is quite difficult to be relaxed to gentle shape. To avoid this kind of breakdown, intermediate piling up was employed in PUFGG. Figure 4 shows x-constant cross section of a grid in the halfway of grid generation. As shown in Fig. 4, 50 layers are piled up in concave region, while only 10 layers are piled up in convex region.

Table 1. Number of cells and Fraction of cell types in ONERA M5 grid (Fig.1-4).

Cell type	Number of cells	Fraction
Tetrahedral	53521	2.9%
Pyramid	60257	3.3%
Prism	317836	17.5%
Hexahedral	1388323	76.3%

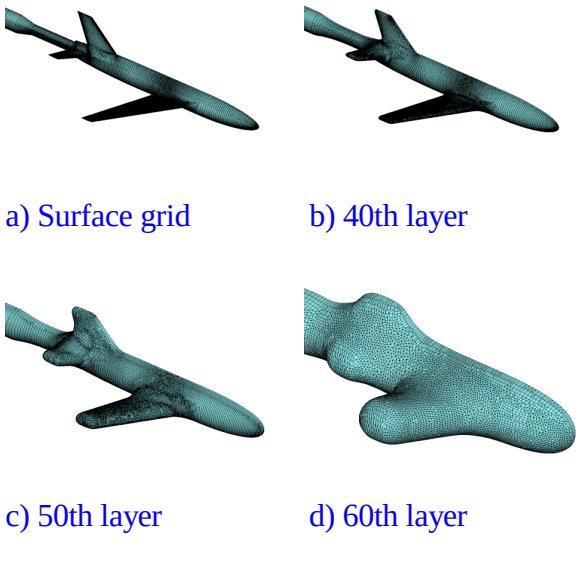

a) Surface grid b) 40th layer

c) 50th layer d) 60th layer

e) 70th layer (0.025scale) f) 105th layer

Fig. 1. Growing volume grid generated by PUFGG.

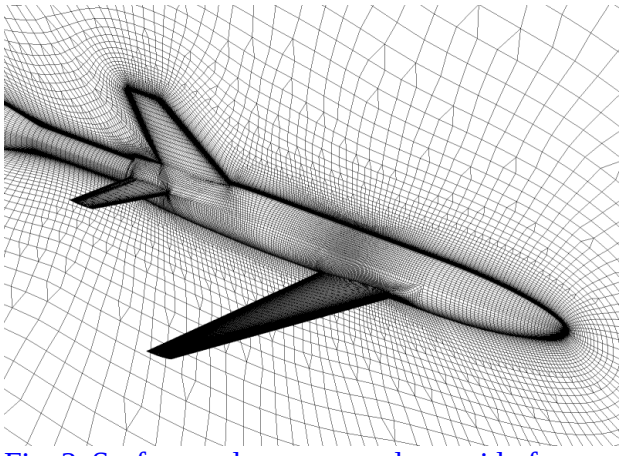

Fig. 2. Surface and symmetry plane grid of ONERA calibration model 5.

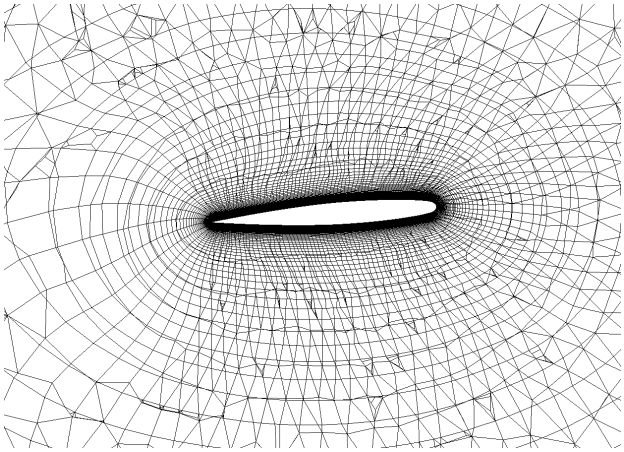

Fig. 3. Grid cross-section at ?=50% location.

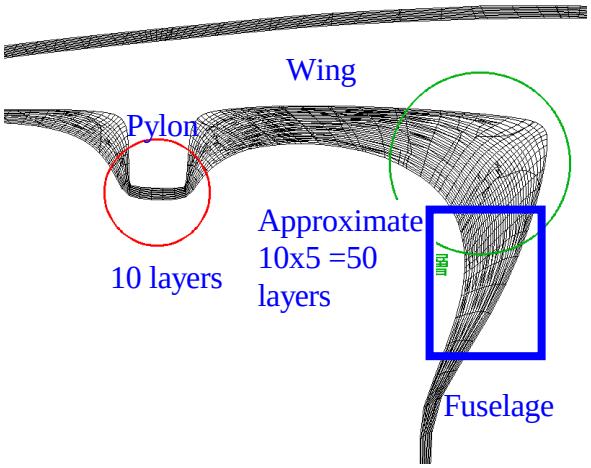

a) Cross section view at x-constant plane for high wing configuration airplane's

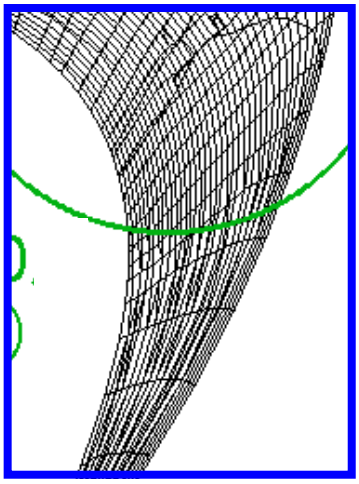

b) Close up view

Fig. 4. Multi stage piling up of volume grid.

4 Flow Solver

In this study, the governing equations are the thin layer approximated Navier-Stokes equations and the Euler equations for viscous and invscid analysis, respectively. UG3 [1] is our own flow solver for viscous and invscid analysis. It is based on unstructured FVM (Finite Volume Method). Spatial discretization is made by MUSCL (Monotone Upwind Scheme for Conservation Laws). Several approximate Riemann solvers are implemented to calculate numerical fluxes. SHUS (Simple High-resolution Upwind Scheme) approximate Riemann solver [2] is used in this study. Time integration is performed by MFGS (Matrix Free Gauss-Seidel method). Several turbulence models are implemented.

UG3 is parallelized using the domain decomposition method and PVM as a message-passing library. Thus it has a good scalability for a wide range of problem size. UG3 can be run on various platform such as PC, PC cluster, UNIX Workstation, UNIX SMP cluster, vector super computer, parallel super computer.

Typical calculation time for viscous analysis of wing-fuselage configuration is about 8 hours using 4 nodes PC cluster.

5 Numerical results

Figure 5 shows Surface and symmetry plane grid of NAL NEXST-1 (scaled model next generation supersonic transport) [3]. Calculation conditions are summarized in Table 2. Pressure coefficient distribution is shown in Fig. 6. Contours are very smooth without unphysical pressure jump that often appears in tetrahedral volume grid system. Cones of the shock wave are clearly captured. Comparison of three component force coefficients between CFD and Wind Tunnel Test (WTT) is plotted in Fig. 7 [4]. CFD results and WTT results show very good agreement. Lift vs. Drag Polar curve is shown in Fig. 8. Agreement between CFD and WTT is also very good.

Table 2. Calculation properties for NEXST-1.

Reynolds number	6.6×10^6
Mach number	2.0
Angle of attack	0.0deg
Number of surface grid cells	17,200 cells
Number of volume grid cells	892,800 cells
Turbulence model	Baldwin-Barth one equation model
Surface grid generation time	1 day (CAD GUI operation)
Volume grid generation	1 hour (PUFGG)
Calculation time	8 hours (PC Cluster; P4 2GHz 4CPU)

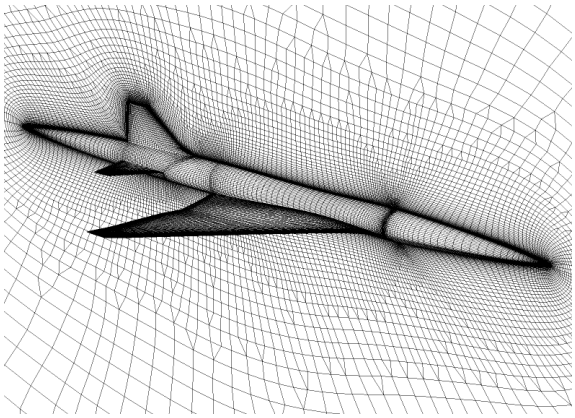

Fig. 5. Surface and symmetry plane grid of NEXST-1

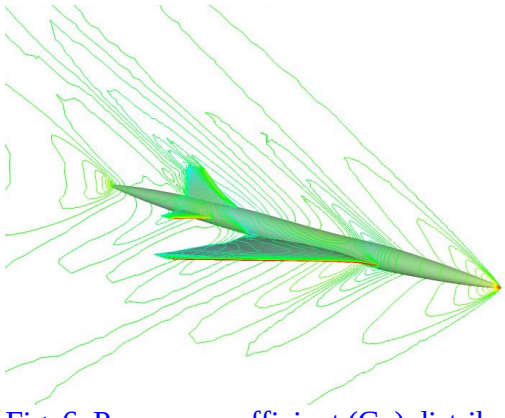

Fig. 6. Pressure coefficient (Cp) distribution of NEXST-1

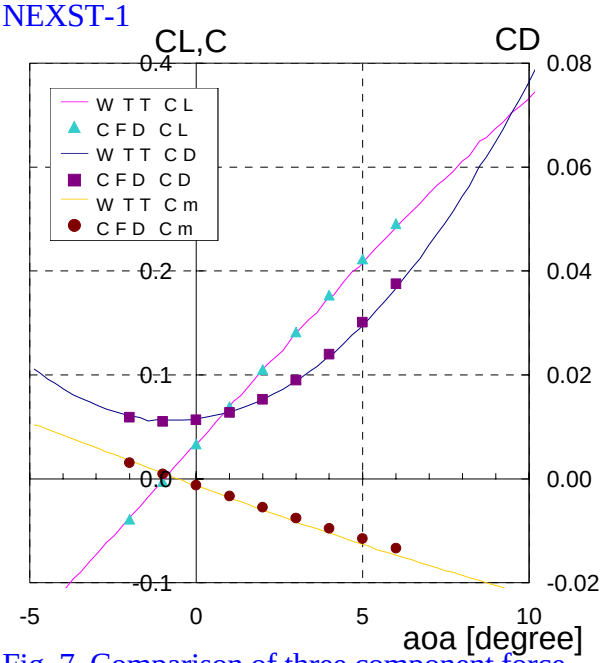

Fig. 7. Comparison of three component force coefficients between CFD and WTT.

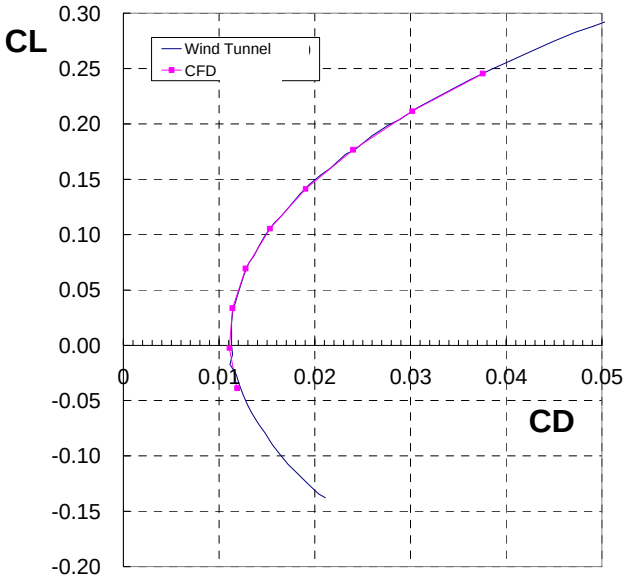

Fig. 8. Comparison of lift vs. drag polar curve.

Figure 9 shows surface pressure coefficient (Cp) distribution for ONERA calibration model 5. Calculation properties are summarized in Table 3. Lift coefficient vs. drag coefficient plot is compared to wind tunnel test in Fig. 10. Agreement between CFD and wind tunnel test is not so good for this case, because turbulence model causes misprediction of shock location. As shown in Fig. 11, Baldwin-Barth (BB) one equation model and Baldwin-Lomax (BL) algebraic model mispredict shock location, while Spalart-Allmaras (SA) one equation model well predicts shock location. Though SA model shows good prediction for shock location, it tends to over predict shock separation at higher angle of attack region at transonic condition. There is no turbulence model that covers all kinds of flow characteristics. Hence CFD results for transonic aircraft is not so reliable that we can blindly accept it. CFD results should be carefully treated especially for aerodynamic design of aircraft that requires highly accurate analysis. Thus there are many factors should being take into account, such as grid, numerical schemes in particular turbulence model, convergence threshold, that affect numerical result.

Table 3. Calculation properties for ONERA M5.

Reynolds number	6.6×10^6
Mach number	0.84
Angle of attack	0.0deg
Number of surface grid cells	28,531 cells
Number of volume grid cells	1,819,937 cells
Turbulence model	Baldwin-Barth one equation model
Surface grid generation time	2 days (CAD GUI operation)
Volume grid generation	1.5 hours (PUFGG)
Calculation time	10 hours (PC Cluster; P4 2GHz 4CPU)

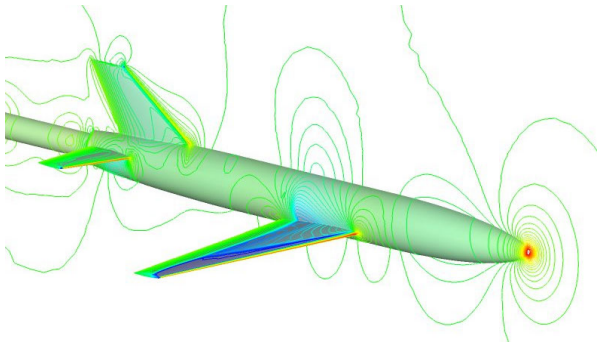

Fig. 9. Pressure coefficient (Cp) contours on surface and symmetry plane of ONERA M5.

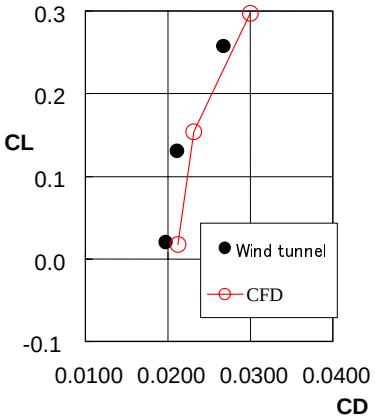

Fig. 10. CL vs. CD plot for ONERA M5 $Re=2.0 \times 10^6$ using Baldwin-Barth turbulence model.

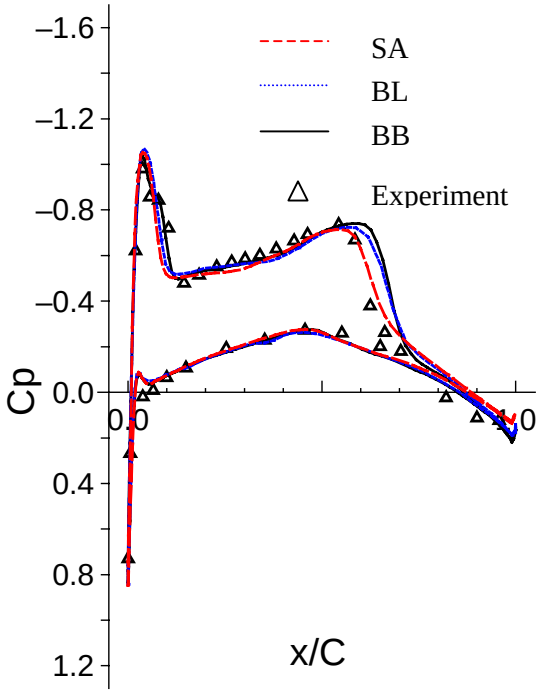

Fig. 11. Comparison of pressure distributions for some turbulence model. ?=30%

Figures 12-15 show numerical grid system generated by PUFGG for BK117 Rotorcraft, which is developed by Kawasaki and MBB (Eurocopter Deutschland). It is too complicated geometry to generate using multi-block structured grid by GUI operation in practical time period. It takes only a week to make numerical grid using the present hybrid grid system start from the CAD/CATIA surface definition data. Main rotor is treated as an actuator disk, which produces pressure jumps between upper and lower side of rotor. Overlapped grid approach is utilized to include main rotor disk in mother grid. Calculation properties are summarized in Table 4.

Surface pressure distribution is shown in Fig. 16. Figure 17 shows streamline. It illustrates wake geometry of main rotor. Wake geometry of main rotor is a major issue to design rotorcraft, because interaction between main rotor wake and fuselage sometimes causes serious vibration and, interaction between main rotor wake and tail rotor generates a loud noise. Figure 18 is the oil flow visualization. This is helpful to design fuselage. In particular to design fairing design, oil flow based design is often applied.

Table 4. Calculation properties for BK117.

Reynolds number	$5x10^6$
Mach number	0.15
Angle of attack	-5.0deg
Number of surface grid cells	41,107 cells
Number of volume grid cells	3,124,542 cells
Turbulence model	Baldwin-Barth one equation model
Surface grid generation time	5 days (CAD GUI operation)
Volume grid generation	3 hours (PUFGG)
Calculation time	30 hours (PC Cluster; P4 2GHz 4CPU)

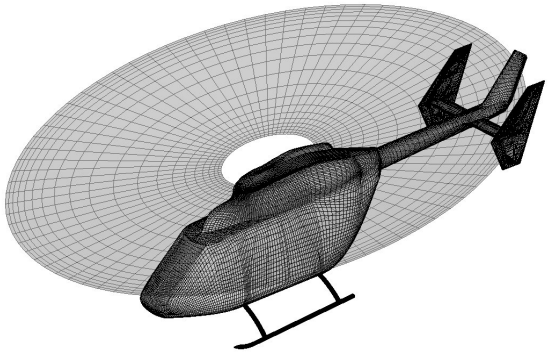

Fig. 12. Surface mesh of BK117 rotorcraft.

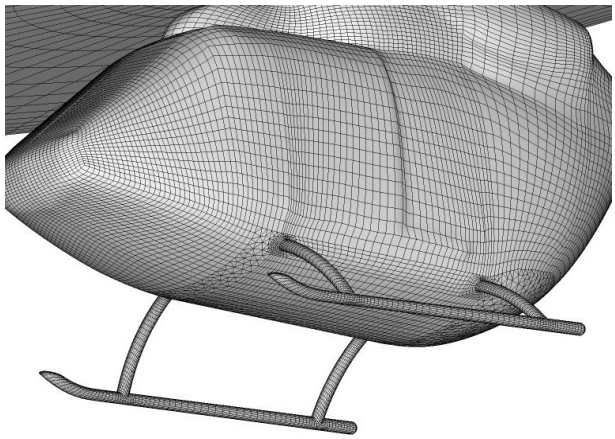

Fig. 13. Close up view of surface mesh of BK117 rotorcraft

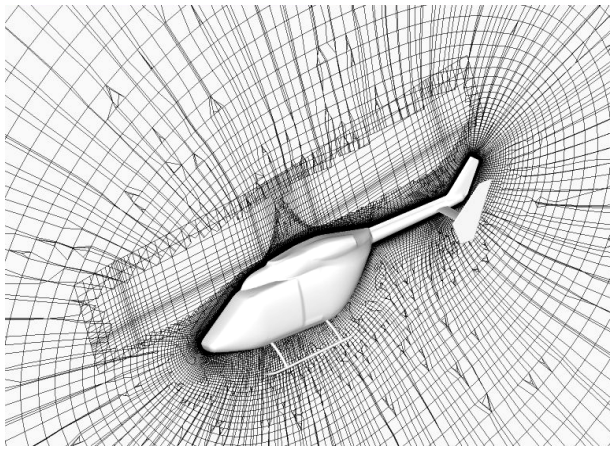

Fig. 14. Cross section view of overlapped grid system at y=0 plane.

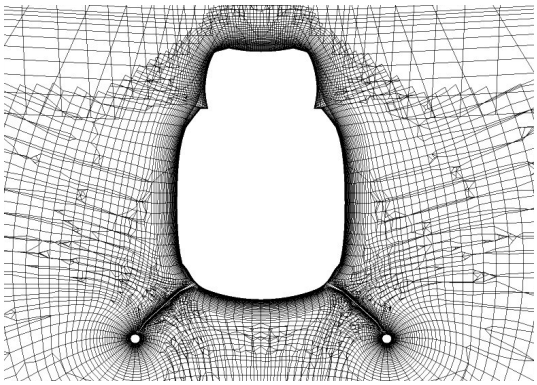

Fig.15. Cross section of overlapped grid system at x=3m plane.

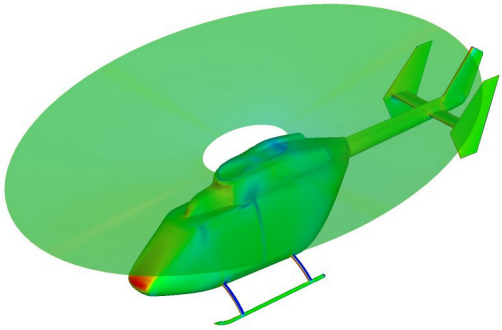

Fig. 16. Surface pressure coefficient (Cp) distribution on BK117 rotorcraft.

Fig. 17. Visualization of streamlines from linear seeds.

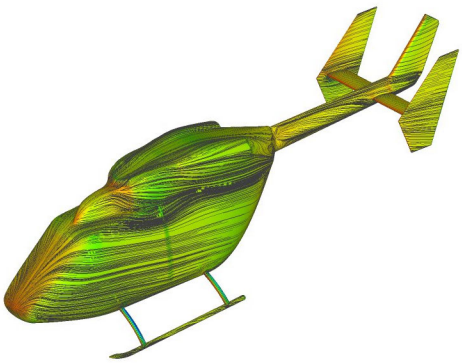

Fig. 18. Visualization of surface streamlines.

Figure 19 presents another case of complex geometry analysis. Surface mesh contains wing, nacelle, and pylon. The automatic grid generator PUFGG can handle this kind of complex geometry.

PUFGG is applicable to the deflection of control surfaces as well. Viscous analysis is performed to deflected aileron using the PUFGG and the UG3 code as shown in Fig. 20.

Figure 21 visualizes distribution of momentum loss for ONERA M5. The momentum loss is observed at shock location on the wing and boundary layer region. Shock induced wave drag can be evaluated by integration of this momentum loss at trailing edge for z-direction over the outside boundary layer region [5]. In contrast, friction drag can be evaluated by integration in same manner over inside boundary layer.

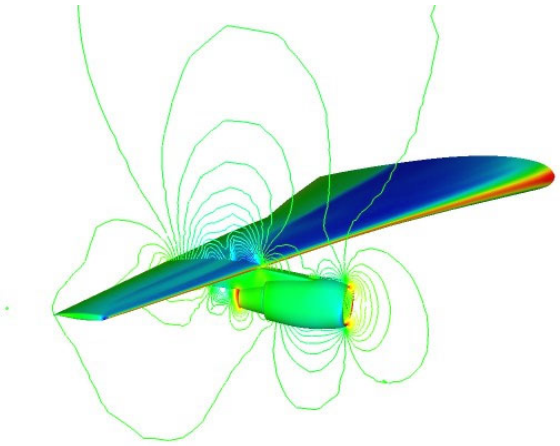

Fig.19. Pressure coefficient (Cp) distributions in wing, nacelle, and pylon configuration.

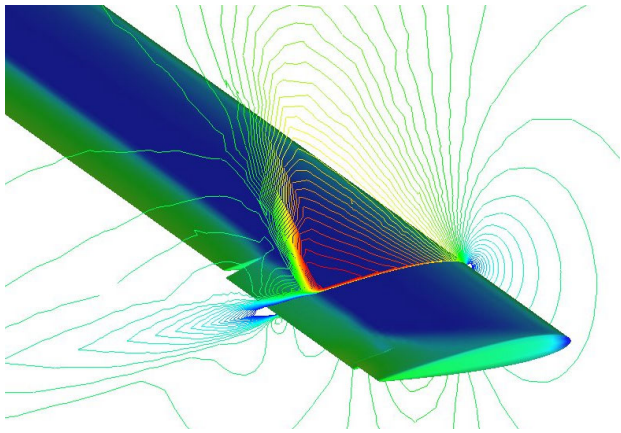

Fig. 20. Surface pressure distribution and Mach number contours for wing with deflected aileron.

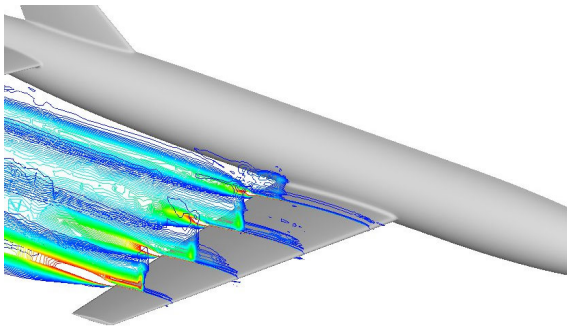

Fig. 21. Visualization of momentum loss for ONERA M5

The last numerical result is a design of wing-fuselage fairing using viscous analysis. Surface streamlines for two types of fairing are compared in Fig. 22. While limiting streamline is appeared for nominal fairing, streamlines on the modified fairing is very smooth. These results are well agreed with oil flow test in wind tunnel. In addition, numerical analysis has other advantage; Reynolds number effect can be taken into account.

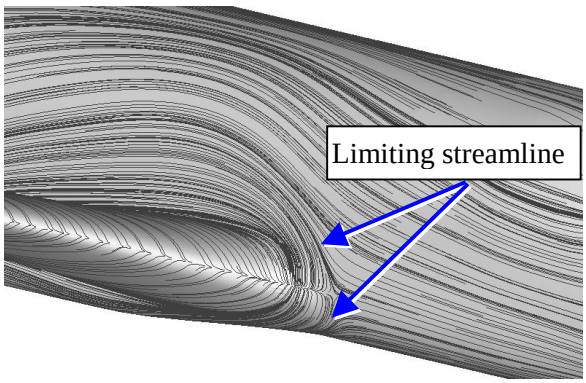

a) Nominal faring

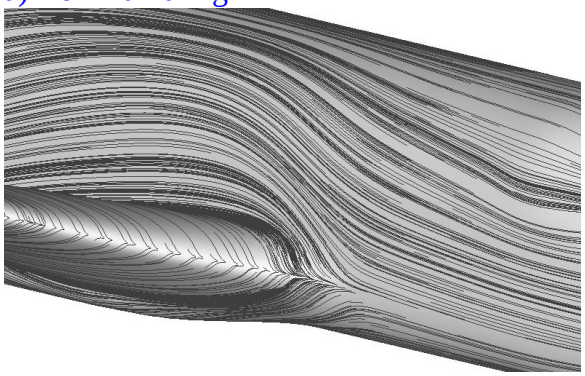

b) Modified faring

Fig. 22. Comparison of oil flow visualization between two wing-fuselage faring.

6 Conclusions

A hybrid grid system and an automatic grid generator were developed. The hybrid grid systems showed good properties to perform aerodynamic analysis with good accuracy and resolution. The automatic grid generator PUFGG developed in this study, significantly reduced grid generation time from a few months to a couple of hours. Especially for highly complex geometry, reduction of turn around time of CFD analysis is significant. It becomes easy to validate the accuracy for realistic shapes. As a result, CFD analysis has been taken more important roll in a development of aircrafts.

In future, factors that affect numerical result such as grid density, numerical schemes in particular turbulence model should be quantitatively assessed. Factors that affect wind tunnel test such as sting interference, aero-elasticity are also assessed to compare between CFD and wind tunnel test in order to validate each other.

References

[1] Shima,E., Ochi,A., Nakamura,T., Saito,S., and Iwamiya,T. Unstructured Grid CFD on Numerical Wind Tunnel, in Parallel Computational Fluid Dynamics, pp.475-482, North Holland, 1999.

[2] Shima,E. and Jounouchi,T. Role of CFD in Aeronautical Engineering(No.14) -AUSM type Upwind Schemes-“, Proceedings of the 14th NAL Symposium on Aircraft Computational Aerodynamics, pp.7-12

[3] Sakata, K. Supersonic Research Program in NAL, Japan, 1st International CFD Workshop for Super-Sonic Transport Design, pp.1-4, 1998.

[4] Ochi, A., Shima, E. A Flow Analysis of the NAL NEXST-1 using Hybrid Unstructured Grid System, 3rd International CFD Workshop for Super-Sonic Transport Design, in printing, 2001.

[5] Lock, R.C. Prediction of the Drag of Wing at Subsonic Speeds by Viscous/Inviscid Interaction Techniques, AGARD-R-723 No.10